THE JOURNAL OF PHYSICAL CHEMISTRY B
A JOURNAL OF THE AMERICAN CHEMICAL SOCIETY

pubs.acs.org/JPCB

Article

Molecular Alignment-Mediated Stick−Slip Poiseuille Flow of Oil in Graphene Nanochannels

Shiwen Wu, Zhihao Xu, Ruda Jian, Siyu Tian, Long Zhou, Tengfei Luo,* and Guoping Xiong*

Cite This: *J. Phys. Chem. B* 2023, 127, 6184−6190

Read Online

ACCESS | Metrics & More | Article Recommendations | Supporting Information

ABSTRACT: The flow behavior of oil in nanochannels has attracted extensive attention for oil transport applications. In most, if not all, of the prior theoretical simulations, oil molecules were observed to flow steadily in nanochannels under pressure gradients. In this study, non-equilibrium molecular dynamics simulations are conducted to simulate the Poiseuille flow of oil with three different hydrocarbon chain lengths in graphene nanochannels. Contrary to the conventional perception of steady flows of oil in nanochannels, we find that oil molecules with the longest hydrocarbon chain (i.e., *n*-dodecane) exhibit notable stick−slip flow behavior. An alternation between the high average velocity of *n*-dodecane in the slip motion and the low average velocity in the stick motion is observed, with a drastic, abrupt velocity jolt of up to 40 times occurring at the transition in a stick−slip motion. Further statistical analyses show that the stick−slip flow behavior of *n*-dodecane molecules originates from the molecular alignment change of oil near the graphene wall. The molecular alignment of *n*-dodecane shows different statistical distributions under stick and slip motion states, leading to significant changes of friction forces and thus notable velocity fluctuations. This work provides new insights into the Poiseuille flow behavior of oil in graphene nanochannels and may offer useful guidelines for other mass transport applications.

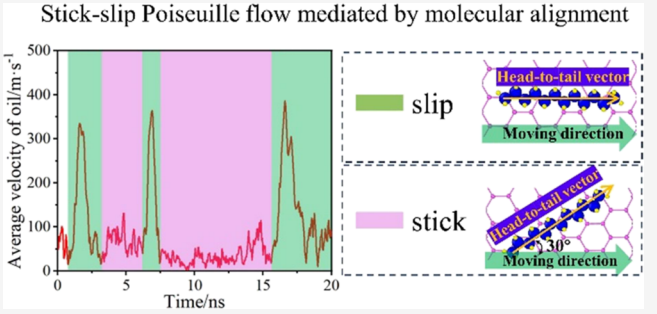

1. INTRODUCTION

With the ever-increasing energy demand globally, the development of oil industry has gained extensive attention.[1,2] Investigating oil transport in porous materials remains one of the most important topics since understanding the flow behavior of oil is crucial to a wide range of applications including oil exploitation and purification.[3−5] Moreover, oil spill and leakage occur frequently during offshore oil production or marine transportation, leading to great economic losses and significant damage to the marine environment. Recovering oil spill also requires fast oil transport in oil skimmers.[6,7] Graphene-based materials have been regarded as promising candidates for efficient oil transport and recovery because of their high porosity and oleophilic/hydrophobic features.[8−10] For instance, in our prior work,[8,9] graphene petal-based oil skimmers with micro- and nanochannels were fabricated to achieve fast continuous oil recovery from oil-contaminated water. However, the underlying physics of oil−graphene interactions remains largely elusive, revealing that the fundamental mechanism is therefore essential to further improve the oil recovery performance of graphene skimmers.

In the past, pressure-driven flows of liquid hydrocarbons in nanochannels have been extensively investigated by molecular dynamics (MD) simulations,[11−20] which are a widely used tool to study fluid transport at the atomic scale. When confined in nanochannels with a width of several molecular layers, oil molecules exhibit unique structures, and intramolecular interactions change dramatically due to the strong interactions between the molecules and the confining channel walls.[21−23] As such, the flow behavior of oil can be changed by adjusting the wall−liquid interactions. For instance, tuning the surface chemistry of channel walls can greatly affect the wall−liquid interactions and thus alter the transport in the channel.[24−26] Moreover, introducing a second phase (e.g., water) has also been proven to efficiently enhance the oil transport rate because of the reduced interactions between oil molecules and the surfaces.[27−29] Among the reported theoretical research on oil transport in nanochannels, oil molecules were observed to flow with negligible velocity fluctuations under a constant driving force or uniform pressure gradient under a steady state. However, the flow behavior of oil in graphene channels is quite complicated and can be affected by many factors such as oil chain length, oil type, and surface chemistry. Investigation of

Received: March 17, 2023
Revised: June 11, 2023
Published: June 27, 2023

https://doi.org/10.1021/acs.jpcb.3c01805
J. Phys. Chem. B 2023, 127, 6184−6190

the fundamental mechanisms governing oil transport in graphene nanochannels is highly warranted.

In this study, systematic MD simulations are conducted to investigate the flow behavior of oil with three different hydrocarbon chain lengths in graphene nanochannels. Contrary to the conventional perception that oil flows steadily in nanochannels under a given pressure gradient, stick−slip flow behavior of oil molecules is observed in graphene nanochannels. Results show that the stick−slip motion depends on the hydrocarbon chain length. Distinct stick−slip motions (velocity jump of up to 40 times) can be observed for oil molecules with the longest hydrocarbon chain of the three chosen oils (i.e., *n*-dodecane), while the average velocity of oil molecules with the shortest hydrocarbon chain, *n*-hexane, barely changes with time (i.e., conventional steady flow). Moreover, we reveal that the stick−slip motion of *n*-dodecane molecules originates from the molecular alignment of oil near the graphene wall, which affects the surface friction forces, and thus leads to notable velocity fluctuations. This work provides new insights into the flow behavior of nanoconfined liquids and will offer useful guidelines for oil transport applications.

2. METHODS AND SIMULATION MODEL

Figure 1a shows a schematic of the simulation setup, in which two graphene layers with a dimension of ∼5 nm (x) × 5 nm

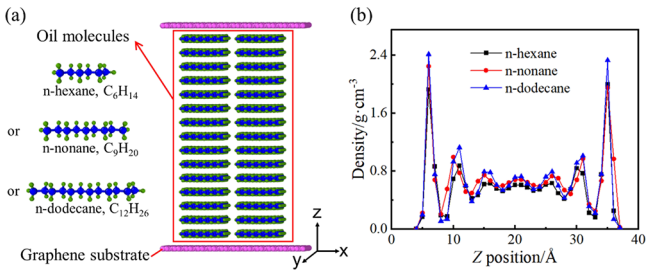

Figure 1. (a) Schematic of the simulation setup in which oil molecules are placed in the graphene channel formed by two graphene layers. Three types of oil, *n*-hexane (C_6H_{14}), *n*-nonane (C_9H_{20}), and *n*-dodecane ($C_{12}H_{26}$), are simulated in this work. (b) Density profiles of equilibrated oil molecules along the *z*-direction.

(y) are used as the channel walls. Periodic boundary conditions are applied in the *x*- and *y*-directions. Three kinds of oil molecules with different lengths of hydrocarbon chains, including *n*-hexane (C_6H_{14}), *n*-nonane (C_9H_{20}), and *n*-dodecane ($C_{12}H_{26}$), are employed to investigate the effect of oil type on the flow behavior in graphene nanochannels. The number of each type of oil molecule is adjusted to maintain the equilibrated channel width at ∼4 nm.

Simulations are performed using the large-scale atomic/molecular massively parallel simulator[30,31] with the time step size chosen to be 1 fs. Oil molecules are modeled using the polymer consistent force field,[32] which has been widely used to simulate a broad range of organic compounds.[33−35] The Tersoff potential is employed to model the interactions between carbon atoms in the graphene substrates.[36] The non-bond interactions between the atoms are simulated by the Lennard−Jones (L−J) potential:[37−40]

$$E = 4\varepsilon\left[\left(\frac{\sigma}{r_{ij}}\right)^{12} - \left(\frac{\sigma}{r_{ij}}\right)^{6}\right] \quad (1)$$

where ε and σ are the energy and length constants, respectively, and r_{ij} is the distance between two atoms i and j. For cross-species pairwise L−J interactions, the Lorentz−Berthelot rule is used:[41,42]

$$\varepsilon_{ij} = \sqrt{\varepsilon_{ii}\varepsilon_{jj}},\ \sigma_{ij} = \frac{\sigma_{ii} + \sigma_{jj}}{2} \quad (2)$$

where σ_{ij} and ε_{ij} are the distance parameters and energy constants of the L−J potential between type i and type j atoms, respectively. All adopted force field parameters are listed in Table 1. A cutoff distance of 12 Å is used for the L−J

Table 1. L−J Potential Parameters for Different Atom Species

	atom	ε (kcal/mol)	σ (Å)
graphene	C	0.055	3.412
oil	C	0.054	4.010
	H	0.02	2.995

interactions. The long-range electrostatic interactions in the entire system are computed by the particle-particle particle-mesh approach[43] with an accuracy of 1×10^{-5}.

First, the system is energy-minimized by the conjugate gradient algorithm to minimize the potential energy of the initial configuration. Subsequently, the system is equilibrated in the isothermal−isobaric ensemble (i.e., NPT) at 300 K and 1 atm for 2 ns, with one side of the graphene channel fixed by a spring force, while the other kept free to move. Oil molecules in the graphene channel can thus achieve the desired pressure of 1 atm. We then fix both sides of the graphene channel and further equilibrate the system in the canonical ensemble (i.e., NVT) at 300 K for another 2 ns. A snapshot of *n*-dodecane molecules in the graphene channel after the equilibration processes is shown in Supplementary Figure S1. To check whether the system has achieved equilibrium, another 3 ns simulation is performed under NVT at 300 K to collect the density profiles of different types of oil along the *z*-direction. As shown in Figure 1b, the average densities of *n*-hexane, *n*-nonane, and *n*-dodecane in the middle region of the graphene channels are calculated to be 0.61, 0.68, and 0.72 g cm^{-3}, respectively, which are closed to the experimental density data for their bulk phases (0.655 g cm^{-3} for *n*-hexane, 0.718 g cm^{-3} for *n*-nonane, and 0.749 g cm^{-3} for *n*-dodecane)[44] at the same pressure and temperature. The results illustrate that these systems have reached equilibrium after the balancing processes.

The flow behavior of oil molecules in the graphene channel is studied by non-equilibrium molecular dynamics (NEMD), which has been widely employed to study the Poiseuille flow of nanoconfined fluids driven by pressure gradients.[45−48] During the simulations, both graphene channel walls are fixed, and constant external driving forces along the *x*-direction are applied to all the oil molecules in the graphene channel to mimic the flow under a constant pressure. Such a method has been widely used to simulate Poiseuille flow.[47,49] The NEMD simulations last for 20 ns, during which the Nosé−Hoover thermostat is applied in the vertical directions of oil flow[48,50] to maintain the simulation temperature at 300 K. The simulations are visualized by the Open Visualization Tool (OVITO).[51]

3. RESULTS AND DISCUSSION

First, the velocities of different types of oil molecules flowing in the graphene nanochannel are calculated and compared under

https://doi.org/10.1021/acs.jpcb.3c01805
J. Phys. Chem. B 2023, 127, 6184−6190

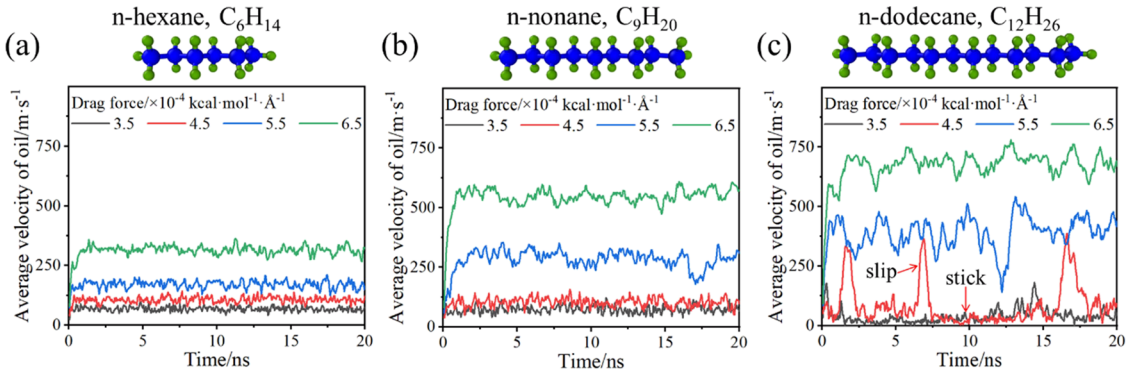

Figure 2. Average velocities of (a) *n*-hexane, (b) *n*-nonane, and (c) *n*-dodecane molecules as functions of the simulation time under different driving forces. *n*-Dodecane oil molecules exhibit apparent stick−slip motion, with the average velocity undergoing drastic, abrupt jumps.

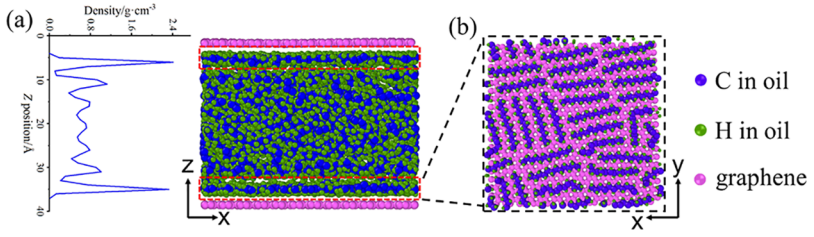

Figure 3. (a) Snapshot of *n*-dodecane molecules in the graphene channel during the Poiseuille flow and the corresponding density profile along the *z*-direction. The red dashed lines show the layered structures of *n*-dodecane near the graphene substrates. (b) *x*−*y* cross-sectional view of one layered structure, in which the molecular chains of *n*-dodecane are aligned parallel to the graphene substrate.

different external driving forces. During each simulation, *x*-component velocities of all the oil molecules are collected and averaged every 100,000 time steps (i.e., 0.1 ns). For each oil type, the average velocities of oil molecules under driving forces ranging from 3.5×10^{-4} to 6.5×10^{-4} kcal mol^{-1} Å^{-1} are plotted as functions of the simulation time, as shown in Figure 2. The corresponding pressure gradients in the nanochannels are calculated and presented in Supplementary Table S1. The results indicate that the average velocity of oil under the same driving force increases with the hydrocarbon chain length, which can be attributed to the lower density of oil with a shorter hydrocarbon chain length. A lower density means a smaller total number of oil atoms in the channel, leading to a lower corresponding pressure on oil and thus a lower velocity under the same driving force. For instance, the corresponding pressure values applied on *n*-hexane (C_6H_{14}) and *n*-nonane (C_9H_{20}) under a driving force of 4.5×10^{-4} kcal mol^{-1} Å^{-1} are 13.4 and 15.12 MPa, respectively, which are lower than that (16.8 MPa) on *n*-dodecane ($C_{12}H_{26}$) under the same driving force (see Supplementary Table S1). Consequently, the average velocity of $C_{12}H_{26}$ molecules surpasses those of the other two types of oil under the same driving force.

Moreover, the average velocities of oil remain relatively stable during the 20 ns simulation for *n*-hexane (C_6H_{14}) molecules under different driving forces. When the length of the hydrocarbon chain increases, the average velocity of oil fluctuates more drastically. In particular, for *n*-dodecane ($C_{12}H_{26}$), oil molecules exhibit apparent stick−slip flow behavior under a driving force of 4.5×10^{-4} kcal mol^{-1} Å^{-1}, with high average velocities (slip) and low average velocities (stick) alternatively showing up for three times during the 20 ns simulation. At the transition of a stick−slip motion, the velocity of oil molecules undergoes drastic, abrupt changes (up to a 40 times difference). The velocity distributions of $C_{12}H_{26}$ molecules within the graphene nanochannel are plotted in Supplementary Figure S2. Notably, the velocity of $C_{12}H_{26}$ molecules remains nearly constant in the near-wall regions with a thickness of 4 Å. In the middle region, the velocity profiles display a parabolic shape with low curvatures. For $C_{12}H_{26}$ molecules in both near-wall and middle regions, the velocities exhibit significantly higher values in the slip motion than in the stick motion. The flow behavior of $C_{12}H_{26}$ molecules under the same driving force but along the *y*-direction is also explored. Results show that $C_{12}H_{26}$ molecules exhibit apparent stick−slip behavior as well when flowing along the *y*-direction (Supplementary Figure S3). Moreover, the magnitude of the velocity jumps is highly dependent on the applied external driving force and the length of the hydrocarbon chain. For instance, although the stick−slip motion of $C_{12}H_{26}$ weakens under higher driving forces, it is still more notable than those of C_6H_{14} and C_9H_{20} molecules under various driving forces.

To understand the underlying fundamental mechanisms of such a stick−slip Poiseuille flow of oil molecules in graphene nanochannels, we investigate the interaction between oil molecules and the channel walls because it can affect the properties of oil molecules at the interface and thus influence the flow behavior. Notably, intense oscillations of oil density can be observed near the graphene walls (Figure 1b), indicating that dense layers of oil are formed in the near-wall regions. Here, taking *n*-dodecane as an example, we visualize the distribution of oil molecules in the graphene channel. Figure 3a presents a snapshot of equilibrated *n*-dodecane molecules in the graphene channel during the Poiseuille flow of *n*-dodecane molecules and the corresponding density profile of oil along the *z*-direction. In the near-wall regions, *n*-dodecane molecules form layered structures with a thickness of ~4 Å, as indicated by the dashed lines. This structural layering

https://doi.org/10.1021/acs.jpcb.3c01805
J. Phys. Chem. B 2023, 127, 6184−6190

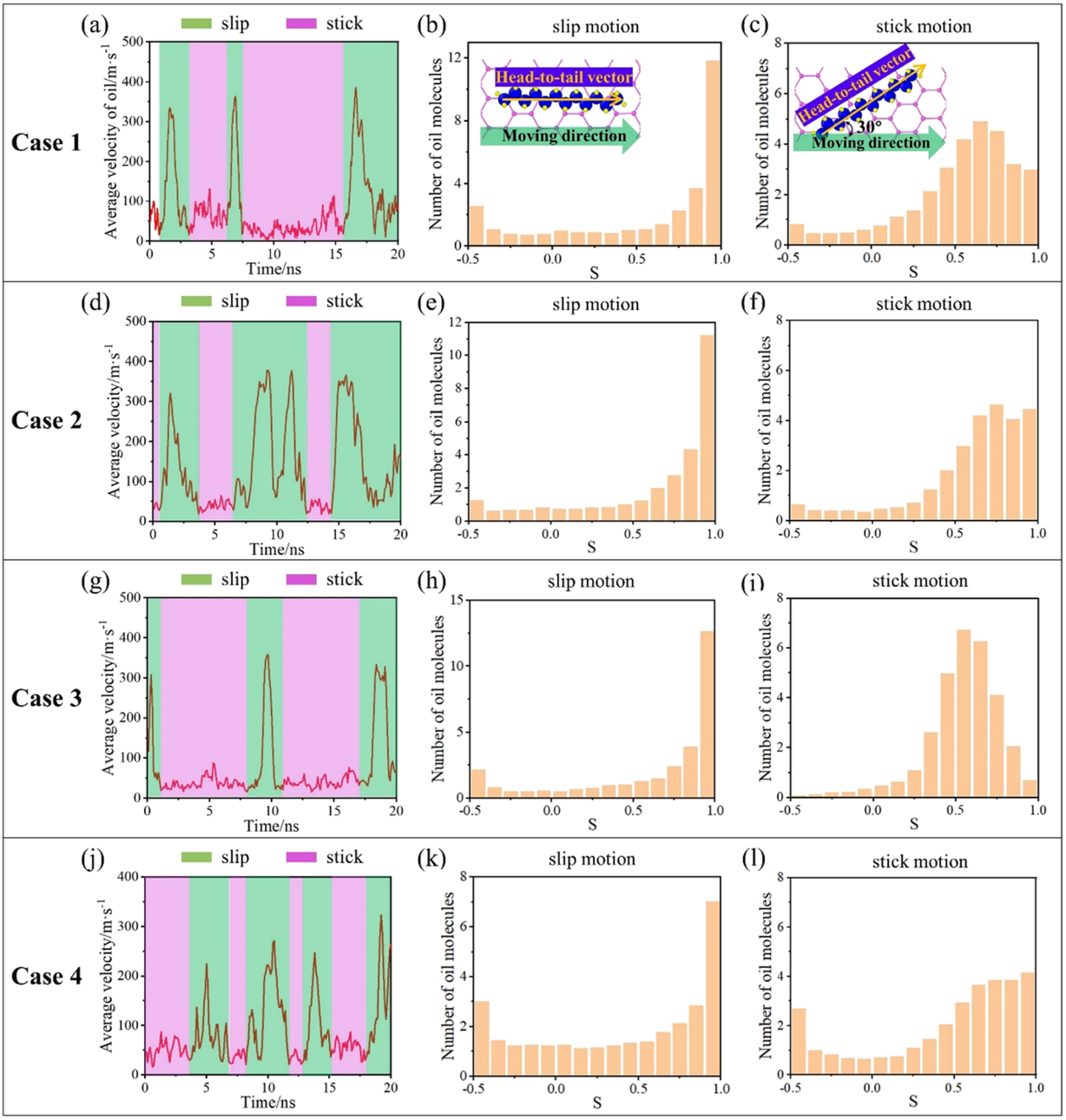

Figure 4. (a) Average velocities of *n*-dodecane molecules as functions of simulation time under a driving force of 4.5×10^{-4} kcal mol^{-1} Å^{-1}. The peaks and valleys of the velocity profile are highlighted, corresponding to the slip and stick motion of *n*-dodecane molecules, respectively. (b) Statistical distribution of *S* of the *n*-dodecane molecules in the layered structure under the slip motion state. (c) Statistical distribution of *S* of the *n*-dodecane molecules in the layered structure under the stick motion state. (d–l) Average velocity profiles and corresponding statistical *S* distributions of *n*-dodecane under slip and stick motion states in repeated simulations.

phenomenon is caused by the strong non-bond solid–liquid interactions[18,52] between *n*-dodecane molecules and graphene substrates. Figure 3b exhibits the *x*–*y* cross-sectional view of one layered structure shown in Figure 3a. The chain-like *n*-dodecane oil molecules are laying parallel to the graphene substrate, with the molecular chains aligned in different directions. Such a phenomenon also occurs in the equilibrium state (i.e., the moment when the balancing processes are completed), as shown in Supplementary Figure S1. Similar layered structures can also be observed in the systems containing *n*-hexane and *n*-nonane molecules (Supplementary Figures S4 and S5). It has also been previously observed that alkanes can form crystal domains as those shown in Figure 3b due to the lattice match between the graphene and the alkane molecules.[53,54] Note that the majority of the carbon chains in the layered structure are aligned straight and in parallel to the graphene wall, which can be attributed to the favorable interfacial interaction energy[55] and the effect of geometric packing.[56,57] A few carbon chains are folded occasionally, potentially caused by thermal vibrations during the simulation.[58] Moreover, the *n*-dodecane molecules display a greater head-to-tail vector length in the near-wall region compared to the middle region of the nanochannel (Supplementary Figure S6), indicating that the *n*-dodecane molecules near the wall are more preferable to be straight than those in the middle region.

https://doi.org/10.1021/acs.jpcb.3c01805
J. Phys. Chem. B 2023, 127, 6184–6190

Will there be any correlation between the orientation of molecular chains in the layered structures and the stick−slip flow behavior of *n*-dodecane oil molecules in graphene channels? To reveal the origin, the orientation parameter (S) of each oil molecule is calculated by:[28,59]

$$S = \frac{3}{2}\cos^2\theta - \frac{1}{2} \tag{3}$$

where θ is the angle between the x axis and the head-to-tail vector of the oil molecule. The value of S ranges from −0.5 to 1. S = 1 represents that the oil molecule is aligned parallel to the flow direction (i.e., x axis), while S = − 0.5 represents that the oil molecule is aligned perpendicular to the flow direction. Under a driving force of 4.5×10^{-4} kcal mol^{-1} Å^{-1}, *n*-dodecane molecules exhibit distinct stick−slip behavior in the Poiseuille flow, with high average velocities during the slip motion and low average velocities under the stick motion alternating for three times within the 20 ns of simulation time (Figure 4a). We calculate the statistical distribution of the averaged S of the *n*-dodecane molecules in the layered structure near the graphene walls under slip and stick motion states separately. As shown in Figure 4b, when the *n*-dodecane molecules are slipping, more oil molecules in the layering structure are aligned parallel to the flow direction (i.e., S = 1). In contrast, the S distribution under the stick motion state exhibits a peak around S = 0.65 (Figure 4c), corresponding to an angle of ∼30° between the molecule and the flow directions. To validate the reliability of such observations, another three repeated simulations (cases 2−4) are conducted. Initially, for each case, we maintain identical simulation settings during the balancing processes, except for extending the processes by random periods of time. As such, at the beginning of the Poiseuille flow, oil molecules have different statistical distributions of properties under identical conditions of temperature and pressure (i.e., 300 K and 1 atm). Subsequently, the same simulation parameters, such as driving forces, are employed in all four cases during the Poiseuille flow processes. As shown in Figure 4d−l, *n*-dodecane molecules in all the three additional simulations exhibit stick−slip motion behavior, and similar statistical S distributions can be observed for the oil molecules during stick and slip motion processes.

The different statistical S distributions of *n*-dodecane under stick and slip motions suggest that the molecular alignment of oil molecules can greatly affect their flow behavior in the graphene channel. We further examine the friction forces between the layered structure and the graphene wall in the four repeated simulations shown in Figure 4. Friction forces are collected through the x-component interaction forces between the graphene substrates and the layered structures at every time step. The friction forces between *n*-dodecane molecules in the layered structure as functions of time in the four simulations are shown in Supplementary Figure S7. Here, the collected friction forces of *n*-dodecane molecules under stick and slip motions in each case (Figure 4a,d,g,j) are averaged. As shown in Figure 5, for all simulations, the friction forces decrease distinctly when the *n*-dodecane molecules are under the slip motion state (i.e., peaks of the velocity profile) and restored to higher values when the *n*-dodecane molecules are under the stick motion state (i.e., valleys of the velocity profile). As such, we can conclude that for *n*-dodecane molecules flowing in the graphene nanochannel, the stick−slip behavior is dependent on the molecular alignment of oil in the near-wall regions. When the oil molecules are aligned along the flow direction, the friction force between the layering structure decreases as the molecules can slide, leading to a high average velocity (i.e., slip motion). In contrast, when the molecules misalign with the flow direction, the molecules in the neighboring layers need to overcome the corrugated landscape, resulting in a lower average velocity (i.e., stick state).

Figure 5. Average friction forces between *n*-dodecane molecules in the layered structure and graphene channels under slip and stick motion states in four repeated simulation cases.

4. CONCLUSIONS

In summary, we have conducted systematic MD simulations to investigate the stick−slip Poiseuille flow behavior of oil molecules in graphene nanochannels. Average velocities of oil molecules with three different lengths of the hydrocarbon chain are collected. Oil molecules with the longest hydrocarbon chain (i.e., *n*-dodecane) studied exhibit distinct stick−slip motions, in which high average velocities under the slip motion state and low average velocities under the stick motion state are observed to appear alternatively, showing apparent velocity jumps (up to 40 times). The magnitude of velocity jumps depends on the external driving force applied to oil molecules. This phenomenon is quite different from the flow behavior of oil with shorter chains and those reported in prior work. The stick−slip oil flow is found to be correlated with the molecular alignment of oil molecules in the near-wall regions. In the slip motion, most of oil molecules in the layered structure are aligned parallel to the flow direction, leading to smaller friction forces and thus higher velocities, while in the stick motion, the statistical molecular alignments of *n*-dodecane molecules in the layered structure exhibit a quasi-normal distribution (i.e., S = 0.65 with an angle of ∼30° between the hydrocarbon chain and the moving direction), resulting in larger friction forces and thus lower velocities. This finding facilitates a better understanding of the Poiseuille flow behavior of nanoconfined oil molecules in graphene channels and may provide new insights into studying the stick−slip motion of molecules in other mass transport applications.

■ ASSOCIATED CONTENT

Supporting Information

The Supporting Information is available free of charge at https://pubs.acs.org/doi/10.1021/acs.jpcb.3c01805.

Snapshots showing different types of oil in the graphene channels, velocity distributions of *n*-dodecane molecules, lengths of head-to-tail vectors of *n*-dodecane molecules, and friction forces between *n*-dodecane molecules and the graphene wall (PDF)

https://doi.org/10.1021/acs.jpcb.3c01805
J. Phys. Chem. B 2023, 127, 6184−6190

AUTHOR INFORMATION

Corresponding Authors

Tengfei Luo − *Department of Aerospace and Mechanical Engineering, University of Notre Dame, Notre Dame, Indiana 46556, United States;* orcid.org/0000-0003-3940-8786; Email: tluo@nd.edu

Guoping Xiong − *Department of Mechanical Engineering, The University of Texas at Dallas, Richardson, Texas 75080, United States*; Email: Guoping.Xiong@utdallas.edu

Authors

Shiwen Wu − *Department of Mechanical Engineering, The University of Texas at Dallas, Richardson, Texas 75080, United States;* orcid.org/0000-0001-8065-0684

Zhihao Xu − *Department of Aerospace and Mechanical Engineering, University of Notre Dame, Notre Dame, Indiana 46556, United States;* orcid.org/0000-0003-1054-3669

Ruda Jian − *Department of Mechanical Engineering, The University of Texas at Dallas, Richardson, Texas 75080, United States*

Siyu Tian − *Department of Mechanical Engineering, The University of Texas at Dallas, Richardson, Texas 75080, United States;* orcid.org/0000-0001-6463-0691

Long Zhou − *Department of Mechanical Engineering, The University of Texas at Dallas, Richardson, Texas 75080, United States*

Complete contact information is available at: https://pubs.acs.org/10.1021/acs.jpcb.3c01805

Notes

The authors declare no competing financial interest.

ACKNOWLEDGMENTS

G.X. thanks the University of Texas at Dallas startup fund and NSF (Grant No. CBET-1949962). T.L. thanks the support from the NSF (Grant No. CBET-1949910). The simulations are supported by the TACC Lonestar6 system.

REFERENCES

(1) Sun, F.; Yao, Y.; Li, G.; Zhang, S.; Xu, Z.; Shi, Y.; Li, X. A Slip-Flow Model for Oil Transport in Organic Nanopores. *J. Pet. Sci. Eng.* **2019**, *172*, 139−148.

(2) Hughes, J. D. A Reality Check on the Shale Revolution. *Nature* **2013**, *494*, 307−308.

(3) Yang, X.; Wang, Z.; Shao, L. Construction of Oil-Unidirectional Membrane for Integrated Oil Collection with Lossless Transportation and Oil-in-Water Emulsion Purification. *J. Membr. Sci.* **2018**, *549*, 67−74.

(4) Kim, S.; Kim, K.; Jun, G.; Hwang, W. Wood-Nanotechnology-Based Membrane for the Efficient Purification of Oil-in-Water Emulsions. *ACS Nano* **2020**, *14*, 17233−17240.

(5) Chen, X.; Dai, C.; Zhang, T.; Xu, P.; Ke, W.; Wu, J.; Qiu, M.; Fu, K.; Fan, Y. Efficient Construction of a Robust PTFE/Al2O3 Hydrophobic Membrane for Effective Oil Purification. *Chem. Eng. J.* **2022**, *435*, No. 134972.

(6) Jernelöv, A. How to Defend against Future Oil Spills. *Nature* **2010**, *466*, 182−183.

(7) Ma, Q.; Cheng, H.; Fane, A. G.; Wang, R.; Zhang, H. Recent Development of Advanced Materials with Special Wettability for Selective Oil/Water Separation. *Small* **2016**, *12*, 2186−2202.

(8) Wu, S.; Yang, H.; Xiong, G.; Tian, Y.; Gong, B.; Luo, T.; Fisher, T. S.; Yan, J.; Cen, K.; Bo, Z.; Ostrikov, K. K. Spill-SOS: Self-Pumping Siphon-Capillary Oil Recovery. *ACS Nano* **2019**, *13*, 13027−13036.

(9) Wu, S.; Tian, S.; Jian, R.; Wu, T.-N.; Milazzo, T. D.; Luo, T.; Xiong, G. Graphene Petal Foams with Hierarchical Micro- and Nano-Channels for Ultrafast Spontaneous and Continuous Oil Recovery. *J. Mater. Chem. A* **2022**, *10*, 11651−11658.

(10) Wu, S.; Jian, R.; Tian, S.; Zhou, L.; Luo, T.; Xiong, G. Simultaneous Solar-Driven Seawater Desalination and Continuous Oil Recovery. *Nano Energy* **2023**, *107*, No. 108160.

(11) Zheng, H.; Du, Y.; Xue, Q.; Zhu, L.; Li, X.; Lu, S.; Jin, Y. Surface Effect on Oil Transportation in Nanochannel: A Molecular Dynamics Study. *Nanoscale Res. Lett.* **2017**, *12*, 413.

(12) Wang, X.; Xiao, S.; Zhang, Z.; He, J. Transportation of Janus Nanoparticles in Confined Nanochannels: A Molecular Dynamics Simulation. *Environ. Sci.: Nano* **2019**, *6*, 2810−2819.

(13) Liu, J.; Yang, Y.; Sun, S.; Yao, J.; Kou, J. Flow Behaviors of Shale Oil in Kerogen Slit by Molecular Dynamics Simulation. *Chem. Eng. J.* **2022**, *434*, No. 134682.

(14) Cui, W.; Shen, Z.; Yang, J.; Wu, S. Molecular Dynamics Simulation on Flow Behaviors of Nanofluids Confined in Nano-channel. *Case Stud. Therm. Eng.* **2015**, *5*, 114−121.

(15) Liu, J.; Zhao, Y.; Yang, Y.; Mei, Q.; Yang, S.; Wang, C. Multicomponent Shale Oil Flow in Real Kerogen Structures via Molecular Dynamic Simulation. *Energies* **2020**, *13*, 3815.

(16) Li, Z.; Yao, J.; Kou, J. Mixture Composition Effect on Hydrocarbon−Water Transport in Shale Organic Nanochannels. *J. Phys. Chem. Lett.* **2019**, *10*, 4291−4296.

(17) Zhan, S.; Su, Y.; Jin, Z.; Wang, W.; Li, L. Effect of Water Film on Oil Flow in Quartz Nanopores from Molecular Perspectives. *Fuel* **2020**, *262*, No. 116560.

(18) Wang, S.; Javadpour, F.; Feng, Q. Molecular Dynamics Simulations of Oil Transport through Inorganic Nanopores in Shale. *Fuel* **2016**, *171*, 74−86.

(19) de Lara, L. S.; Michelon, M. F.; Miranda, C. R. Molecular Dynamics Studies of Fluid/Oil Interfaces for Improved Oil Recovery Processes. *J. Phys. Chem. B* **2012**, *116*, 14667−14676.

(20) Cao, Z.; Jiang, H.; Zeng, J.; Saibi, H.; Lu, T.; Xie, X.; Zhang, Y.; Zhou, G.; Wu, K.; Guo, J. Nanoscale Liquid Hydrocarbon Adsorption on Clay Minerals: A Molecular Dynamics Simulation of Shale Oils. *Chem. Eng. J.* **2021**, *420*, No. 127578.

(21) Mozaffari, S.; Tchoukov, P.; Mozaffari, A.; Atias, J.; Czarnecki, J.; Nazemifard, N. Capillary Driven Flow in Nanochannels − Application to Heavy Oil Rheology Studies. *Colloids Surf., A* **2017**, *513*, 178−187.

(22) Lu, H.; Xu, Y.; Duan, C.; Jiang, P.; Xu, R. Experimental Study on Capillary Imbibition of Shale Oil in Nanochannels. *Energy Fuels* **2022**, *36*, 5267−5275.

(23) Liu, B.; Wu, R.; Baimova, J. A.; Wu, H.; Law, A. W.-K.; Dmitriev, S. V.; Zhou, K. Molecular Dynamics Study of Pressure-Driven Water Transport through Graphene Bilayers. *Phys. Chem. Chem. Phys.* **2016**, *18*, 1886−1896.

(24) Zhang, H.-H.; Wang, B.-B.; Xu, Z.-M.; Li, X.-C.; Yan, W.-M. Molecular Dynamics Simulation on Evaporation Enhancement of Water and Aqueous Nano-Films by the Application of Alternating Electric Field. *Int. J. Heat Mass Transfer* **2019**, *145*, No. 118735.

(25) Wang, Y.; Yu, X.; Wan, X.; Yang, N.; Deng, C. Anomalous Impact of Surface Wettability on Leidenfrost Effect at Nanoscale. *Chin. Phys. Lett.* **2021**, *38*, No. 094401.

(26) Yang, L.; Wan, X.; Ma, D.; Jiang, Y.; Yang, N. Maximization and Minimization of Interfacial Thermal Conductance by Modulating the Mass Distribution of the Interlayer. *Phys. Rev. B* **2021**, *103*, No. 155305.

(27) Zhan, S.; Su, Y.; Jin, Z.; Zhang, M.; Wang, W.; Hao, Y.; Li, L. Study of Liquid-Liquid Two-Phase Flow in Hydrophilic Nano-channels by Molecular Simulations and Theoretical Modeling. *Chem. Eng. J.* **2020**, *395*, No. 125053.

(28) Zhang, W.; Feng, Q.; Jin, Z.; Xing, X.; Wang, S. Molecular Simulation Study of Oil-Water Two-Phase Fluid Transport in Shale Inorganic Nanopores. *Chem. Eng. Sci.* **2021**, *245*, No. 116948.

(29) Liu, H.; Xiong, H.; Yu, H.; Wu, K. Effect of Water Behaviour on the Oil Transport in Illite Nanopores: Insights from a Molecular Dynamics Study. *J. Mol. Liq.* **2022**, *354*, No. 118854.

(30) Plimpton, S. Fast Parallel Algorithms for Short-Range Molecular Dynamics. *J. Comput. Phys.* **1995**, *117*, 1−19.
(31) Wu, S.; Huang, D.; Yu, H.; Tian, S.; Malik, A.; Luo, T.; Xiong, G. Molecular Understanding of the Effect of Hydrogen on Graphene Growth by Plasma-Enhanced Chemical Vapor Deposition. *Phys. Chem. Chem. Phys.* **2022**, *24*, 10297−10304.
(32) Sun, H.; Mumby, S. J.; Maple, J. R.; Hagler, A. T. An Ab Initio CFF93 All-Atom Force Field for Polycarbonates. *J. Am. Chem. Soc.* **1994**, *116*, 2978−2987.
(33) Luo, T.; Lloyd, J. R. Enhancement of Thermal Energy Transport Across Graphene/Graphite and Polymer Interfaces: A Molecular Dynamics Study. *Adv. Funct. Mater.* **2012**, *22*, 2495−2502.
(34) Sengupta, S.; Pant, R.; Komarov, P.; Venkatnathan, A.; Lyulin, A. V. Atomistic Simulation Study of the Hydrated Structure and Transport Dynamics of a Novel Multi Acid Side Chain Polyelectrolyte Membrane. *Int. J. Hydrogen Energy* **2017**, *42*, 27254−27268.
(35) Gamba, M.; Kovář, P.; Pospíšil, M.; Torres Sánchez, R. M. Insight into Thiabendazole Interaction with Montmorillonite and Organically Modified Montmorillonites. *Appl. Clay Sci.* **2017**, *137*, 59−68.
(36) Yarahmadi, A.; Hashemian, M.; Toghraie, D.; Abedinzadeh, R.; Ali Eftekhari, S. Investigation of Mechanical Properties of Epoxy-Containing Detda and Degba and Graphene Oxide Nanosheet Using Molecular Dynamics Simulation. *J. Mol. Liq.* **2022**, *347*, No. 118392.
(37) Huang, D.; Wu, S.; Xiong, G.; Luo, T. Effect of Electric Field on Water Free Energy in Graphene Nanochannel. *J. Appl. Phys.* **2022**, *132*, No. 015104.
(38) Wu, S.; Xu, Z.; Tian, S.; Luo, T.; Xiong, G. Enhanced Water Evaporation under Spatially Gradient Electric Fields: A Molecular Dynamics Study. *J. Mol. Liq.* **2022**, *360*, No. 119410.
(39) Pan, D.-K.; Zong, Z.-C.; Yang, N. Phonon Weak Couplings in Nanoscale Thermophysics. *Acta Phys. Sin.* **2022**, *71*, No. 086302.
(40) Zong, Z.-C.; Pan, D.-K.; Deng, S.-C.; Wan, X.; Yang, L.-N.; Ma, D.-K.; Yang, N. Mixed Mismatch Model Predicted Interfacial Thermal Conductance of Metal/Semiconductor Interface. *Acta Phys. Sin.* **2023**, *72*, 034401−034401.
(41) Tian, S.; Huang, D.; Xu, Z.; Wu, S.; Luo, T.; Xiong, G. Enhanced Thermal Transport across the Interface between Charged Graphene and Poly(Ethylene Oxide) by Non-Covalent Functionalization. *Int. J. Heat Mass Transfer* **2022**, *183*, No. 122188.
(42) Tian, S.; Xu, Z.; Wu, S.; Luo, T.; Xiong, G. Anisotropically Tuning Interfacial Thermal Conductance between Graphite and Poly(Ethylene Oxide) by Lithium-Ion Intercalation: A Molecular Dynamics Study. *Int. J. Heat Mass Transfer* **2022**, *195*, No. 123134.
(43) Pang, Y.; Zhang, J.; Ma, R.; Qu, Z.; Lee, E.; Luo, T. Solar−Thermal Water Evaporation: A Review. *ACS Energy Lett.* **2020**, *5*, 437−456.
(44) Rumble, J. *CRC Handbook of Chemistry and Physics*, 2017.
(45) Kumar Kannam, S.; Todd, B. D.; Hansen, J. S.; Daivis, P. J. Slip Length of Water on Graphene: Limitations of Non-Equilibrium Molecular Dynamics Simulations. *J. Chem. Phys.* **2012**, *136*, No. 024705.
(46) Kannam, S. K.; Todd, B. D.; Hansen, J. S.; Daivis, P. J. Slip Flow in Graphene Nanochannels. *J. Chem. Phys.* **2011**, *135*, 144701.
(47) Chen, B.; Jiang, H.; Liu, X.; Hu, X. Observation and Analysis of Water Transport through Graphene Oxide Interlamination. *J. Phys. Chem. C* **2017**, *121*, 1321−1328.
(48) Xu, T.; Zhang, M.; Xu, Z.; Yang, X. Molecular Insight into Water Transport through Heterogeneous GO-Based Two-Dimensional Nanocapillary. *ACS Appl. Mater. Interfaces* **2019**, *11*, 33409−33418.
(49) Wei, N.; Peng, X.; Xu, Z. Breakdown of Fast Water Transport in Graphene Oxides. *Phys. Rev. E* **2014**, *89*, No. 012113.
(50) Jiang, C.; Ouyang, J.; Wang, L.; Liu, Q.; Wang, X. Transport Properties and Structure of Dense Methane Fluid in the Rough Nano-Channels Using Non-Equilibrium Multiscale Molecular Dynamics Simulation. *Int. J. Heat Mass Transfer* **2017**, *110*, 80−93.
(51) Stukowski, A. Visualization and Analysis of Atomistic Simulation Data with OVITO−the Open Visualization Tool. *Modell. Simul. Mater. Sci. Eng.* **2010**, *18*, No. 015012.
(52) Tang, J.; Qu, Z.; Luo, J.; He, L.; Wang, P.; Zhang, P.; Tang, X.; Pei, Y.; Ding, B.; Peng, B.; Huang, Y. Molecular Dynamics Simulations of the Oil-Detachment from the Hydroxylated Silica Surface: Effects of Surfactants, Electrostatic Interactions, and Water Flows on the Water Molecular Channel Formation. *J. Phys. Chem. B* **2018**, *122*, 1905−1918.
(53) Bourque, A. J.; Rutledge, G. C. Heterogeneous Nucleation of an N-Alkane on Graphene-like Materials. *Eur. Polym. J.* **2018**, *104*, 64−71.
(54) Liu, Y. F.; Yang, H.; Zhang, Z. M.; Zhang, H. Molecular Dynamics Simulations on the Orientation of N-Alkanes with Different Lengths on Graphene. *Surf. Sci.* **2019**, *690*, No. 121468.
(55) Smith, P.; Lynden-Bell, R. M.; Smith, W. The Behaviour of Liquid Alkanes near Interfaces. *Mol. Phys.* **2000**, *98*, 255−260.
(56) Hu, H.-W.; Carson, G. A.; Granick, S. Relaxation Time of Confined Liquids under Shear. *Phys. Rev. Lett.* **1991**, *66*, 2758−2761.
(57) Wu, K.; Chen, Z.; Li, J.; Lei, Z.; Xu, J.; Wang, K.; Li, R.; Dong, X.; Peng, Y.; Yang, S.; Zhang, F.; Chen, Z.; Gao, Y. Nanoconfinement Effect on N-Alkane Flow. *J. Phys. Chem. C* **2019**, *123*, 16456−16461.
(58) Zhang, T.; Luo, T. High-Contrast, Reversible Thermal Conductivity Regulation Utilizing the Phase Transition of Polyethylene Nanofibers. *ACS Nano* **2013**, *7*, 7592−7600.
(59) Sui, H.; Zhang, F.; Wang, Z.; Wang, D.; Wang, Y. Molecular Simulations of Oil Adsorption and Transport Behavior in Inorganic Shale. *J. Mol. Liq.* **2020**, *305*, No. 112745.

https://doi.org/10.1021/acs.jpcb.3c01805
J. Phys. Chem. B 2023, 127, 6184−6190